Understanding Ultrafast Dynamics of Conformation Specific Photo-Excitation: A Femtosecond Transient Absorption and Ultrafast Raman Loss Study

Journal:	*The Journal of Physical Chemistry*
Manuscript ID	jp-2017-03893f
Manuscript Type:	Article
Date Submitted by the Author:	25-Apr-2017

Complete List of Authors:	Roy, Khokan; Indian Institute of Science (IISc), Department of Inorganic and Physical Chemistry (IPC) Kayal, Surajit; Indian Institute of Science, Dept. of Inorganic and Physical Chemistry Ravi Kumar, Venkatraman; Indian Institute of Science, Dept. of Inorganic and Physical Chemistry Beeby, Andrew; University of Durham, Department of Chemistry Ariese, Freek; VU university, LaserLab Umapathy, Siva; Indian Institute of Science, Inorganic and PhysicalChemistry

Understanding Ultrafast Dynamics of Conformation Specific Photo-Excitation: A Femtosecond Transient Absorption and Ultrafast Raman Loss Study

Khokan Roy,[†] Surajit Kayal, [†] Venkatraman Ravi Kumar, [†] Andrew Beeby,[ǂ] Freek Ariese,[#] and Siva Umapathy[*†‡]

[†]Department of Inorganic and Physical Chemistry, Indian Institute of Science, Bangalore, 560012, India.

[ǂ]University of Durham, Department of Chemistry, South Road, Durham DH1 3LE, U.K.

[#]on leave from LaserLaB, VU University Amsterdam, De Boelelaan 1081, 1081 HV Amsterdam, Netherlands.

[‡]Department of Instrumentation and Applied Physics, Indian Institute of Science, Bangalore, 560012, India.

Corresponding Author
[*]**E-mail:** umapathy@ipc.iisc.ernet.in

Keywords: Conformational isomers, excited state planarization, transient absorption, species associated spectra, Franck-Condon activity, vibrational cooling, time-resolved stimulated Raman.

Abstract:

Excited state ultrafast conformational reorganization is recognized as an important phenomenon that facilitates light-induced functions of many molecular systems. This report describes the femtosecond and picosecond conformational relaxation dynamics of middle-ring and terminal ring twisted conformers of the acetylene π-conjugated system bis(phenylethynyl)benzene, a model system for molecular wires. Torsional effects of the phenyl rings on the ground state electronic structure have been studied with the help of calculated Franck-Condon absorption spectra at different twist angles of the middle phenyl ring. Through excitation wavelength dependent fs-transient absorption measurements, we have shown that the middle-ring and terminal ring twisted conformers relax at femtosecond (400-600 fs) and picosecond (20-24 ps) timescales, respectively. Actinic pumping into the red flank of the absorption spectrum leads to excitation of primarily planar conformers, and results in very different excited state dynamics. In addition, ultrafast Raman loss spectroscopic studies reveal the vibrational mode dependent relaxation dynamics for different excitation wavelengths. Finally, we show that the middle-ring twisted conformer undergoes femtosecond torsional planarization dynamic, whereas the terminal rings relax in few tens of picosecond timescale.

1. Introduction:

Understanding the excited state optical properties of small organic molecules is important for many areas of science and technology, including their potential application in molecular optoelectronics.[1-19] As compared to their inorganic analogues, they are relatively easy to synthesize at lower cost and they are gaining further attention because of their potential applications in nano scale physics.[20-27] A wide range of small organic molecules is currently under spectroscopic investigation by many groups. Examples of this class of molecules include linear pi-conjugated systems with acetylene bridges, ethyl bridges, phenyl bridges, heterocyclic aromatic bridges, etc.[28] Such systems have potential applications in organic light emitting diode (OLEDs), organic light-emitting transistors (OLETs), stable multilevel organic memory devices (OMDs), organic field effect transistors (OFETs) and in organic photovoltaics (OPVs) where light energy is converted to electric energy. Moreover, the molecular geometry in both the ground and excited state plays a vital role in controlling the optical properties of such systems. The specific design of such systems allows tuning their HOMO-LUMO gap from the deep UV to the NIR region, which is useful for generating whitelight.

In this report, we discuss the excited-state structural dynamics of bis(phenylethynyl)benzene (BPEB) (see figure 1a), a cylindrical pi-conjugated system having acetylene linkers that connect the aromatic phenyl rings. Such systems (also known as molecular wires) are well known for their high fluorescence quantum yield (~ 0.7-0.9).[29-30] In the ground state, the rotational barrier about the CC single bonds that connect the acetylene linkers and phenyl rings is of the order of kT.[30-32] Therefore, at

room temperature all possible torsional conformers, with either the middle-ring twisted (MRT) or one of the terminal ring twisted (TRT), will be present at significant levels. Such a wide distribution of rotational isomers makes the ground state absorption spectrum rather broad, although some vibronic structure can still be discerned.[32-33] The excited state structure of BPEB is still elusive because the transient absorption (TA) spectra are even broader. A time-resolved fluorescence study by Beeby and coworkers showed that the fluorescence intensity of the blue part of the fluorescence spectra increases up to 50 ps.[29] This unusual behavior was attributed to structural reorganization

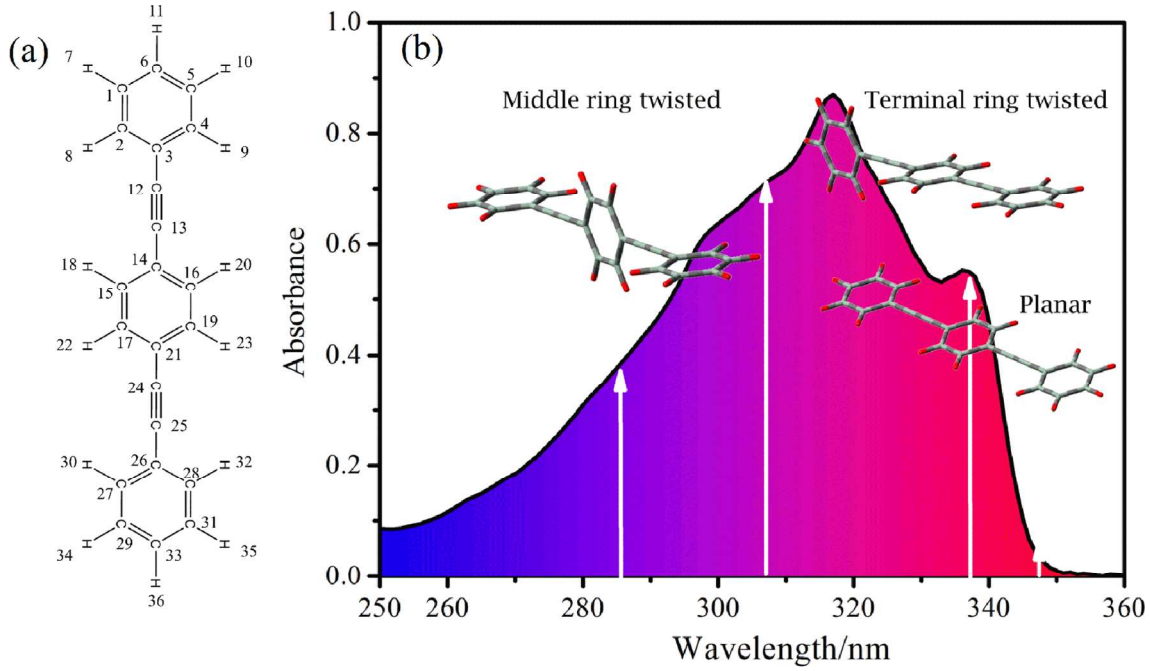

Figure 1. (a) Molecular structure of BPEB drawn in planar conformer. (b) Room temperature absorption spectrum of BPEB (20 μM in acetonitrile) showing the excitation wavelengths as discussed in this paper. The molecular tube structures illustrate the various twisted conformers. For selective excitation of the most planar conformers we used 337 nm for URLS and 347 nm for TA.

of the Franck-Condon state after electronic excitation. Time-resolved picosecond Raman band intensities also showed a gradual increase in intensity with time up to 50-60 picosecond during the excited state evolution of BPEB after photo-excitation at 267 nm.[29]

Our previous report on time-resolved TA and ultra-fast Raman loss spectroscopy (URLS) of BPEB upon 307 nm photo-excitation concerns the multi-exponential kinetic behavior observed in different solvents.[34] The longest lifetime component obtained from femtosecond TA was consistent with the fluorescence lifetime (~500-600 ps) reported in the literature.[29, 34] The time dependent integrated peak area/intensity of three major Raman bands (2126 cm^{-1}, 1573 cm^{-1} and 1130 cm^{-1} modes) showed a biphasic increase, as concluded from transient URLS measurements for the same excitation wavelength. This biphasic behavior after photo excitation at 307 nm was assigned to two phases of planarization. Vibrational frequencies of a few major Raman bands, i.e., CC double bond and CC triple bond stretches, showed a redshift at sub-picosecond timescales, followed by a slower blueshift at tens of picoseconds timescales. The initial redshift is due to the ultrafast relaxation from the initially excited Franck-Condon geometry.[35-37] On the other hand, the slow rise (~ 20-24 ps) is assigned to vibrational relaxation (vibrational cooling) of high frequency vibrations, coupled to torsional relaxation of the terminal and central phenyl rings. The kinetics were very complex because at room temperature BPEB exists as a mixture of conformers, that can all be excited at 307 nm. Therefore, in this paper we have decided to explore the effect of different pump wavelengths to selectively excite different populations of conformers.

In this current report, we discuss the origin of the two phases of planarization of optically excited BPEB. Along with TA and URLS with selective excitation, a computational study (Franck-Condon analysis) was also carried out to obtain structural insight into the complex nature of the excited state geometry of BPEB. The room temperature absorption spectrum of BPEB is quite broad in solution phase where the

vibronic structure is less evident, as shown in figure 1b. Our computational studies (vide infra) show that conformers with the three phenyl rings in the same plane could produce an absorption spectrum that is quite similar to the low temperature absorption spectrum reported by Chu and Pang.[38] Gradual twisting of the central phenyl ring produces a room temperature absorption spectrum. So, the red part of the absorption spectrum contains nearly planar or planar structures exclusively, while the blue part of the spectrum contains both terminal and central ring twisted structures. Therefore, for this work, the excitation pump pulse was chosen in such a way so that it can selectively excite different conformers. At 285 nm the photo pump excites predominantly the twisted conformers, while at 347 nm it can selectively excite the (nearly) planar, minimum energy conformers. We subsequently measured the ultrafast excited-state dynamics of these different populations of conformers in order to observe the effect of the starting conformations on the S_1 decay dynamics of this acetylene pi-conjugated system. The excited-state dynamics of these different sub-sets of populations are discussed using both fs-TA and transient URLS results.

2. Experimental and computational methods:

2.1. Ground state absorption studies:

Bis(phenylethynyl)-benzene was prepared via the Sonogashira coupling reaction and the purity was tested as reported earlier.[34] The ground state absorption spectrum of BPEB was recorded using a Shimadzu UV-Vis Spectrophotometer, model UV-2600 at 20 μM concentration in acetonitrile in a 1-cm path length quartz cuvette. The absorption was processed using UVprobe-2.50 software which is supplied as standard with the

spectrophotometer. The spectral range was set from 250-700 nm with a sampling interval of 1 nm and a spectral bandwidth of 2 nm. A reference spectrum was first collected using only solvent and auto zero. All studies were performed at room temperature. Figure 1b shows the absorption spectrum of 20 μM BPEB in acetonitrile solvent at room temperature (25^0C). The peak at 337 nm corresponds to the 0→0 transition for planar rotamers, while the peaks at 316 nm and 306 nm can be related to a combination of vibronic progressions as suggested by Chu and Pang [38] and also due to the existence of a mixture of twisted ground state conformers as depicted in figure 1b.

2.2. Femtosecond TA and transient URLS spectroscopy:

Details of the experimental setup have been described previously.[34] Briefly, femtosecond transient absorption and URLS spectroscopy were performed using a home-built setup [39-40], composed of a Millennium Pro Nd:YVO_4 laser, Tsunami oscillator, Empower Q switched laser, Regenerative amplifier, OPA (Optical Parametric Amplifier), TOPAS (Travelling Optics Optical Parametric Amplifier) and double-array CCD detection system fitted to a 550 Triax monochromator. The Millennium Pro laser is pumped by a diode and after internal frequency doubling gives 532 nm output with 4.6 W power. This output is utilized to pump the Ti-sapphire crystal in a Tsunami Oscillator. The oscillator is a mode-locked laser which produces 790 nm output with 82 MHz repetition rate and 700 mW average power (energy per pulse is ~8.5 nJ). The oscillator output energy per pulse is not sufficient to perform ultrafast experiments. This issue was resolved by reducing the repetition rate of the seed pulse with a Q-switched nanosecond Empower laser which runs at a 1 kHz repetition rate. This Empower laser pumps the

regenerative amplifier. It amplifies the seed pulse to 2 mJ with a 1 kHz repetition rate. This output is utilized for multiple purposes: 1 mJ is used to generate a visible range of wavelengths (480-780 nm) from a frequency converter optical parametric amplifier (OPA). This wavelength is used for picosecond Raman pump generation. From the remaining output, 960 µJ is used to pump TOPAS, another frequency converter which can generate light pulses from 230 nm to 2600 nm wavelength with sufficient output energy. This frequency converter is used as photo pump to excite the compound of interest. For this work, the excitation wavelengths generated were 285, 337, and 347 nm, with output energies of 2-5 µJ. The remaining 40 µJ of the 790 nm fundamental is used to

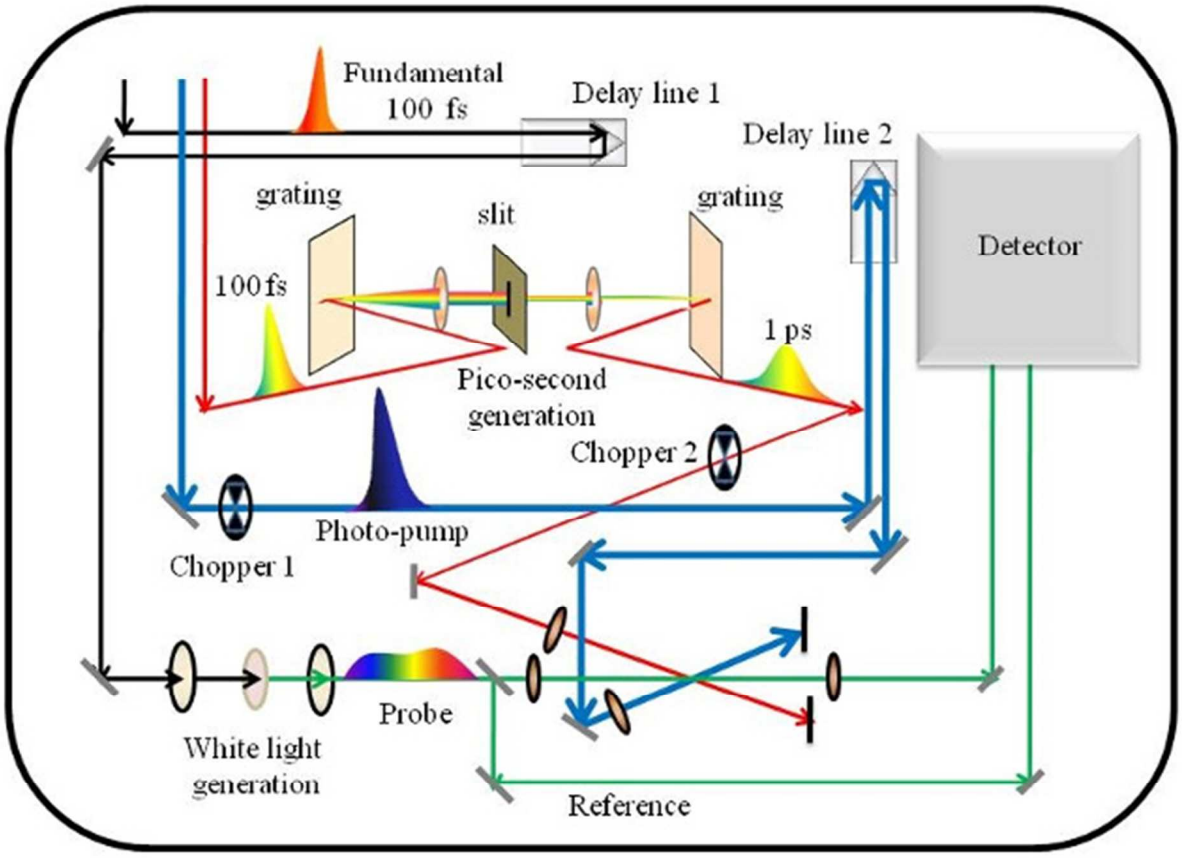

Figure 2. Schematic diagram of experimental set-up for femtosecond transient absorption and ultrafast Raman loss spectroscopy.

generate a whitelight super-continuum broadband probe pulse (420-750 nm). For TA, a magic angle pump-probe geometry was adopted to avoid any rotational diffusion contribution to the kinetic trace. A half-wave plate was used in the pump beam path to achieve the magic angle (54.7°) geometry with respect to the broadband probe beam. For URLS spectroscopy (a technique analogous to stimulated Raman scattering) an extra picosecond narrowband Raman pump pulse created by a 4f-grating pair configuration was utilized in combination with the actinic pump and broadband whitelight. This three pulse combination probes the excited state vibrational structure of the transient species. The picosecond pulse (having 1 ps pulse duration and 14 cm^{-1} spectral bandwidth) being narrow in the frequency domain provides the spectral resolution and the Cross correlation of actinic pump and whitelight probe determines the time resolution of the transient Raman experiment.[39-52] A schematic diagram for both TA and URLS measurements is given in figure 2.

2.3. Computations:

2.3.1. Geometry optimization and FC spectrum simulation:

The ground state structure of BPEB was optimised with the B3LYP/cc-pVDZ method with integral equation formalism-polarizable continuum solvent model [53-59] as implemented in Gaussian 09 (G09) suite.[60] The excited state structure of BPEB was optimized with time dependent-density functional theoretical formalism [61-62] as employed in G09 suite with the same method as for the ground state. Frequency analysis with harmonic approximation was performed on the optimized ground state and excited state structures of BPEB and no imaginary frequencies were obtained indicating that the

optimized structures correspond to local minima. The Franck-Condon (FC) spectrum simulations were performed (as implemented in G09 [63-65]) for different torsional angles (C4-C3-C14-C16 and C19-C21-C26-C28 in anti-clockwise direction) i.e. from 0 – 20 degrees in steps of 5. The FC spectra were simulated by rigid scanning along the torsional angle (described above) in the ground state and for a fixed optimized structure in the excited state to observe the conformational dependence on the FC spectrum. The FC stick spectra (not shown) were convoluted with a Gaussian profile to account for solvent inhomogeneous broadening with a full width half maximum value of 270 cm^{-1} as employed in G09.

3. Results:

Torsional angle dependent vibrationally resolved electronic spectra:

Generally, electronic absorption spectra are simulated by calculating the vertical excitation energies of the optimized ground state geometry.[66-70] This procedure yields stick spectra (infinitesimally small line width) which can be convoluted with user defined Gaussian or Lorentzian functions of a definite line width. By adopting the Franck-Condon principle (nuclei are fixed in position coordinate during electronic transitions) for calculating the transitions between two vibronic states.[71] Thus the simulated spectra by computing the transitions between vibronic states are shown in figure 3. It is evident that for the 0 degree twist (twist angle refers to the twisting angle of the middle-ring with respect to the terminal rings) in the ground state, the simulated vibronic spectrum matches with that of the low temperature experimental absorption

spectra reported by Chu and Pang *et al*., where the 0-0 band is more intense than the other

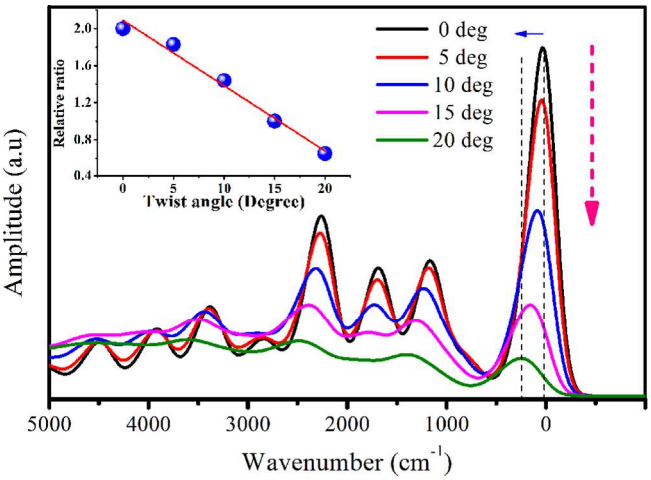

Figure 3. Simulated ground state absorption spectra of BPEB at increasing twist angles of the central ring. The x-axis shows the transition energy relative to the 0-0 transition of the planar species, found experimentally at 28902 cm^{-1} (346 nm). Inset shows the decrease in ratio of two most intense bands.

bands.[38]

On the other hand, the simulated spectrum for 20 degrees twist appears closer to the room temperature absorption spectrum, where the 0-0 band is less intense as compared to the shorter wavelength bands (see figure 3 and figure 1b). This result implies that the room temperature absorption spectrum corresponds to the mixtures of conformers. The inset of figure 3 shows a decrease in the ratio of the 0-0 band intensity relative to that of the main vibronic band at around 2200 cm^{-1} away from the 0-0 band (as shown in figure 3) , as a function of the twist angle of the middle phenyl ring. Further, we observe a blue shift of the 0-0 band on going from planar to twisted conformers as shown in figure 3. So, excitation at different positions of the absorption spectrum with the actinic pump pulse would selectively excite different populations of conformers. Another important observation made from the Franck-Condon analysis concerns the band

assignments of the absorption spectra. A previous assignment was given by Chu and Pang [38], who interpreted the fine structure in the low temperature absorption (and emission) spectra as a progression series of about 1100 cm^{-1}. This was done by subtracting each value from the next higher value in wavenumber. However, if it is done by subtracting from the 0-0 transition only, it yields reasonable numbers that match with the calculated high frequency vibrations and with the excited state Raman bands. These values along with their assignments are shown in Table 1.

Table.1.Vibronic bands obtained from the literature [38] and from our simulated absorption spectrum (as shown in Fig.3)

Literature value (-198˚ C) from low temperature absorption study				Computation (scaled frequencies)	
λ_{max}(nm)	$\bar{\upsilon}$ (cm^{-1})	$\Delta\bar{\upsilon}^a$(cm^{-1})	$\Delta\bar{\upsilon}^b$(cm^{-1})	$\Delta\bar{\upsilon}^b$(cm^{-1})	Modes assignment
346	28902	----	----	----	0-0 transition
333	30030	1128	1128	1096	central ring C-H scissoring
328	30488	458	1586	1601	central ring CC double bond str.
322	31056	568	2154	2169	CC triple bond str. also [(central ring C-H scissoring)+2 quanta] (progression)
----	----	----	----	2744	central ring CC double bond str. + central ring C-H scissoring (combination)
312	32051	995	3149	3242	CC triple bond str. + central ring C-H scissoring, (combination) also 2 quanta of CC double bond (progression)
----	----	----		3770	CC triple bond str. + central ring CC double bond str. (combination)
----	----	----		4338	CC triple bond str. + (2 quanta) (progression)

[a] energy gap here is the difference between each level and its next lower level in wavenumber (from exp. results of ref. 38).

[b] energy gap of vibronic transitions from the 0-0 transition (from exp. results of ref. 38).

Bond lengths in the ground and excited optimized geometry:

If we consider the planar conformer, the symmetry of the molecule is the same (C_{2h}) in both ground and excited states considering that all the phenyl rings are in the same plane. In the ground state optimized geometry, the three phenyl rings have a benzenoid structure and hence the electron cloud is delocalized over the rings. However, there is a variation in bond length due to the effect of the acetylene moieties attached to the phenyl rings. This causes the C_{14}-C_{16} bond length to be 1.414 Å and the C_{16}-C_{19} bond to be 1.390 Å, as shown in Table 2. This effect becomes much more pronounced in the excited state optimized geometry, which is quite different from the ground state. The two terminal rings maintain the benzenoid structure but the central phenyl ring adopts a much

Table 2. Calculated bond lengths of ground state and excited state optimized geometries.

	Ground state	Excited state
Bonds	Bond length (Å)	Bond length (Å)
C3-C4	1.413	1.430
C4-C5	1.395	1.390
C5-C6	1.400	1.410
C3-C12	1.429	1.398
C12-C13	1.222	1.245
C13-C14	1.426	1.390
C14-C16	1.414	1.445
C16-C19	1.390	1.370

more quinoidal structure in the excited state optimized geometry (also see figure S1 in the Supporting Information). The C_{14}-C_{16} bond length increases from 1.414 Å to 1.445 Å,

whereas, the C_{16}-C_{19} bond length decreases from 1.390 Å to 1.370 Å as compared to the ground state geometry. The C_{13}-C_{14} bond that connects the central phenyl ring and the acetylene moiety becomes stronger and shorter, from 1.426 (ground state) to 1.390 Å in the excited state equilibrium geometry. Other bond lengths are given in Table 2. The MOs depict the electron density of BPEB in the ground and excited states, similar to the literature.[29] The excited state MOs show a more quinoidal structure which is not observed in the ground state (see figure S2 in Supporting Information).

Transient Absorption measurements:

Femtosecond transient absorption measurements of BPEB were carried out for different excitation wavelengths. This study was performed in acetonitrile solution at room temperature at 200 μM concentration in a 1-mm pathlength cuvette. As discussed above, the blue edge of the spectrum consists mostly of twisted conformers and the red edge consists almost exclusively of planar conformers, where all phenyl rings are in the same plane, therefore the two selected excitation wavelengths were 285 nm and 347 nm. We note that the results obtained for 307 nm excitation have been reported earlier.[34] The transient absorption spectra recorded for different time delays are shown in figure 4. The spectra are rather broad in nature for 285 nm excitation as compared to 347 nm excitation as shown in figure 4 a & d. It is observed that the absorption maximum λ_{max} is around 620 nm along with a shoulder at 550 nm (ΔE = 2150 cm^{-1}), which could be a vibronic progression of the CC triple bond stretch vibration. Transient spectra for 285 nm excitation show a distinct rise until 50 ps (figure 4a), which is not very prominent for 347 nm excitation (figure 4d and 4e). Another important observation concerns the spectral changes at ultrafast timescales as depicted in figure 4 b & e. It is evident that the initial

TA spectrum (b) at 0.1 ps is quite broad and contains a shoulder around 550 nm which becomes sharper with time. The ultrafast redshift of the blue flank of the TA spectrum is clearly visible after normalization, as shown in figure 4c. This redshift is not observed for 347 nm excitation, as shown in figure 4e and 4f (normalized). At longer time delays around 1000 ps, a triplet species appears as a shoulder at 500 nm which is consistent with literature reports.[29] The measured transient kinetics for all wavelengths and all time

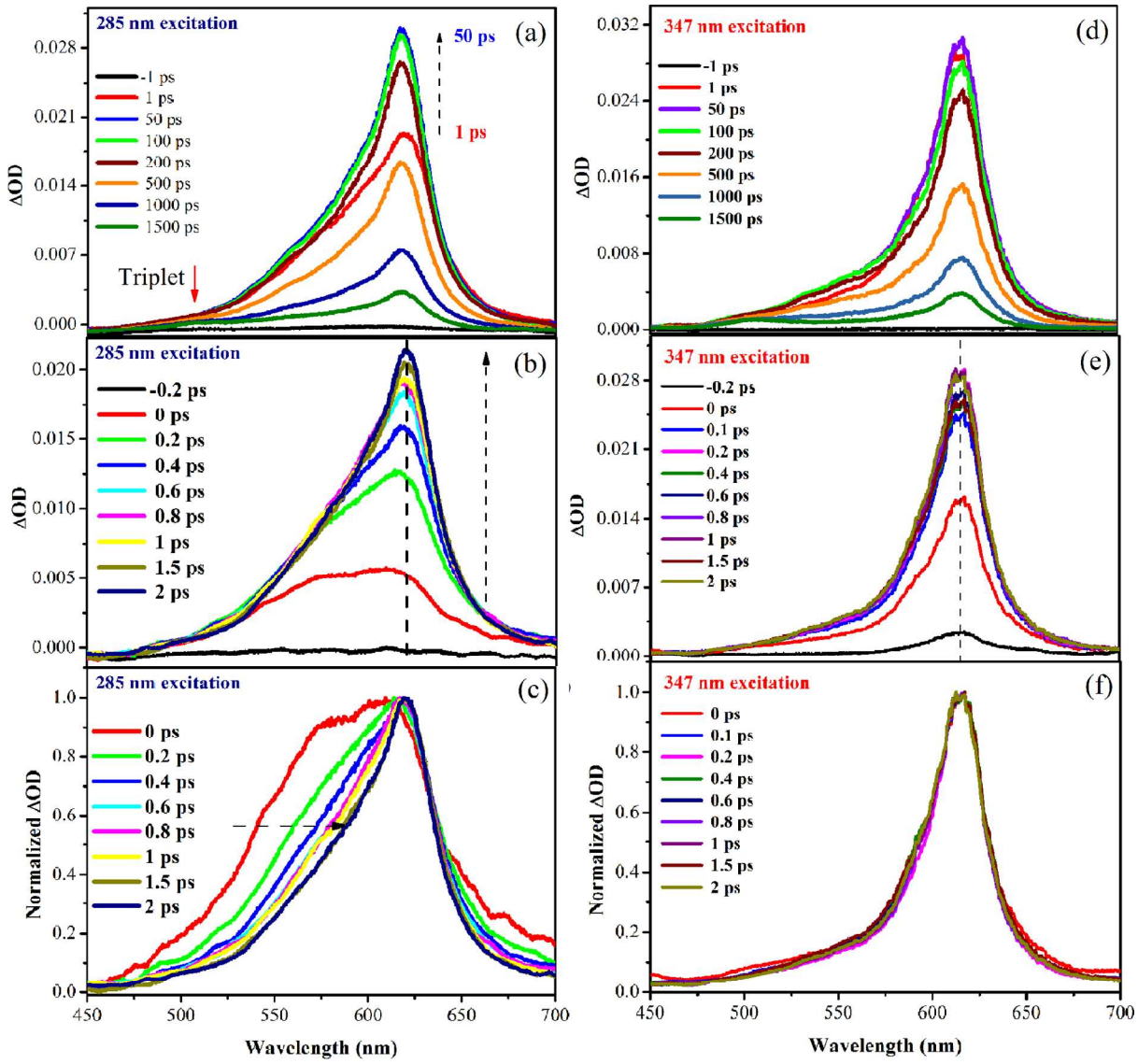

Figure 4.Femtosecond transient absorption spectra of BPEB for two different excitations are shown for longer (top) and shorter delays (middle). The latter are also shown after normalization (bottom frames).

points were fitted globally using tri-exponential functions and de-convoluted with the instrument response function (kinetic traces for few wavelengths along with their exponential fitting are shown in figure S3 in the supporting information). Global fitting for 285 nm yields three time constants: 0.4-0.6 ps, 20-24 ps and 515-567 ps, which is consistent with our previous report.[34] The corresponding species associated spectra obtained from global analysis are shown in figure 5a. The first component is blue shifted and broader as compared to the other two components and the observed amplitude is relatively low. The time constant associated with this ultrafast component is 0.4-0.6 ps. The spectral features and the λ_{max} of the other two components are very similar (Fig. 5a) except that the time constant of to the 2nd component is 20-24 ps (see Table 3). However, the 3rd species decays with a longer time scale, ~515-570 ps, which is consistent with the fluorescence lifetime of the BPEB molecule in solution phase.[29]

Excitation at the very red edge of the absorption spectrum (at 347 nm) yields quite different results (Fig. 5b). The spectral features are similar, but the global analysis yields two time constants: the first component is of ~ 20 ps with a very limited population

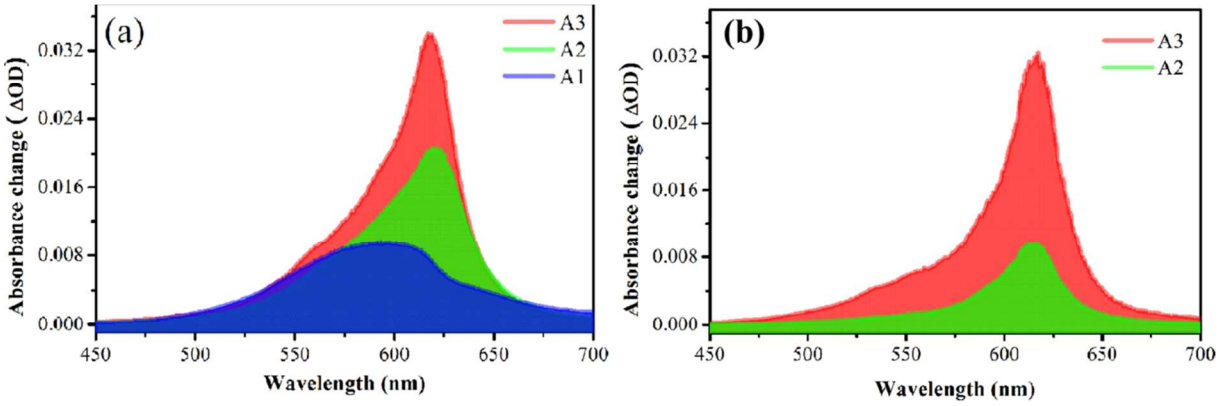

Figure 5. Species associated spectra of TA kinetics after global analysis using tri (285 nm exc, a) and bi (347 nm exc, b) exponential models.

contribution as shown in figure 5b and the second component is of~ 537 ps. This is consistent with 285 nm and 307 nm excitation, except that the ultrafast component is absent. The time constants obtained for different excitations are given in Table 3.

Table 3. Rate constants obtained from global analysis of the TA spectra for three different excitation wavelengths.

Excitation wavelength	Time constant (A) (±100 fs)	Time constant (B) (±4 ps)	Time constant (C) (±50 ps)
285 nm	400 fs	24 ps	569 ps
307[a] nm	600 fs	20 ps	515 ps
347 nm	----	20 ps	537 ps

[a]Data from our previous report.[34]

Transient Raman measurements:

For ultrafast stimulated Raman scattering, the excited state resonance condition was utilized to achieve a sufficient signal-to-noise ratio. The excited state Raman signals were detected in URLS mode at the anti-Stokes side of the whitelight probe for different time delays. The transient Raman spectra contain several high frequency vibrations such as CC triple and CC double bond stretches and inner and outer phenyl ring CH bending vibrations. All these vibrations are highly Franck-Condon active and have been assigned in our previous report.[34] The excited state Raman spectra for the different time delays are shown in figure 6 for the 285 nm and the 337 nm excitations. We note that the red edge

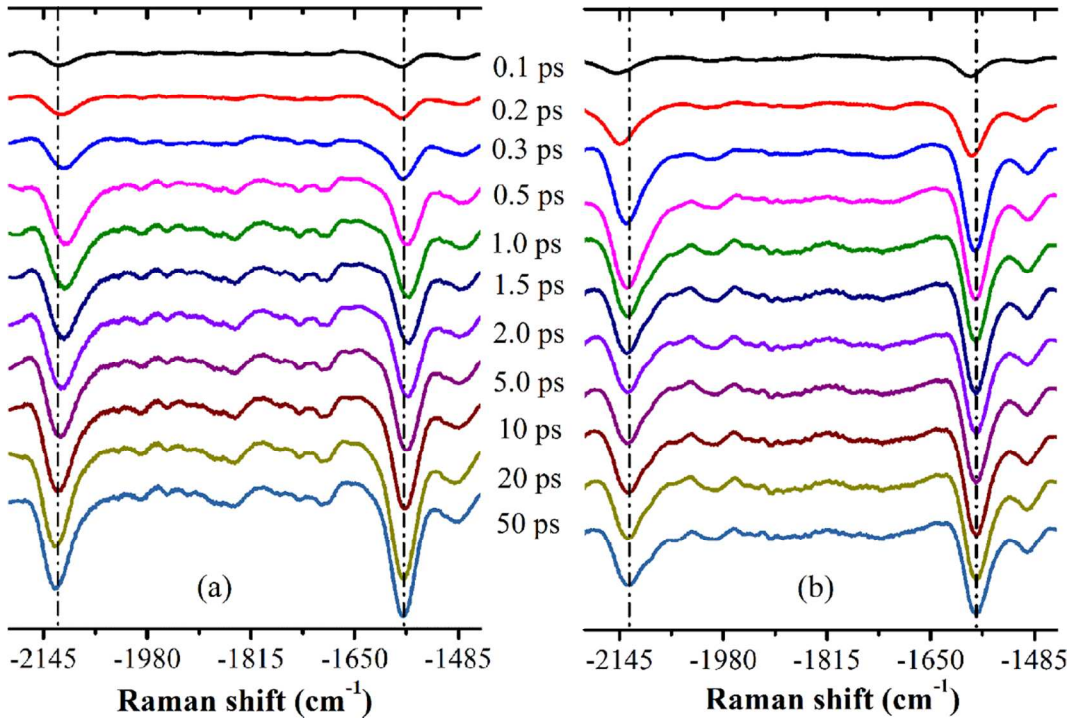

Figure 6. Transient Raman loss spectra of BPEB for 285 nm (a) and 337 nm (b) excitation wavelength at different time delays showing the CC double and triple bond stretches. Vertical lines are guides to the eye.

excitation wavelength for Raman was chosen at 337 nm instead of 347 nm (used for TA) in order to obtain a better signal-to-noise ratio (owing to higher resonance absorbance, see figure 1b). The URLS spectra at 347 nm excitation (not shown) were much noisier, but otherwise similar to the 337 nm results. Again, these excitation wavelengths were chosen to excite mostly the highly twisted conformers (in case of 285 nm) or the (nearly) planar conformers (in case of 337 nm excitation). Analysis of the URLS Raman peak positions for the 285 nm excitation of the high frequency vibrations (−C≡C− and >C═C<) shows an initial redshift until about one picosecond, and at longer timescales it shows a blue shift over a few tens of picoseconds which is also consistent with our previous report at 307 nm excitation.[34] These red and blue shifts are exponential in nature as shown in figure 7a for 285 nm excitation. Double exponential fitting of this time dependent peak position gives a ~0.1-0.2 ps time constant for the red-shift and 12-16 ps

for the blue-shift in case of the CC triple bond and 20-21 ps in case of the CC double bond stretching vibrations.

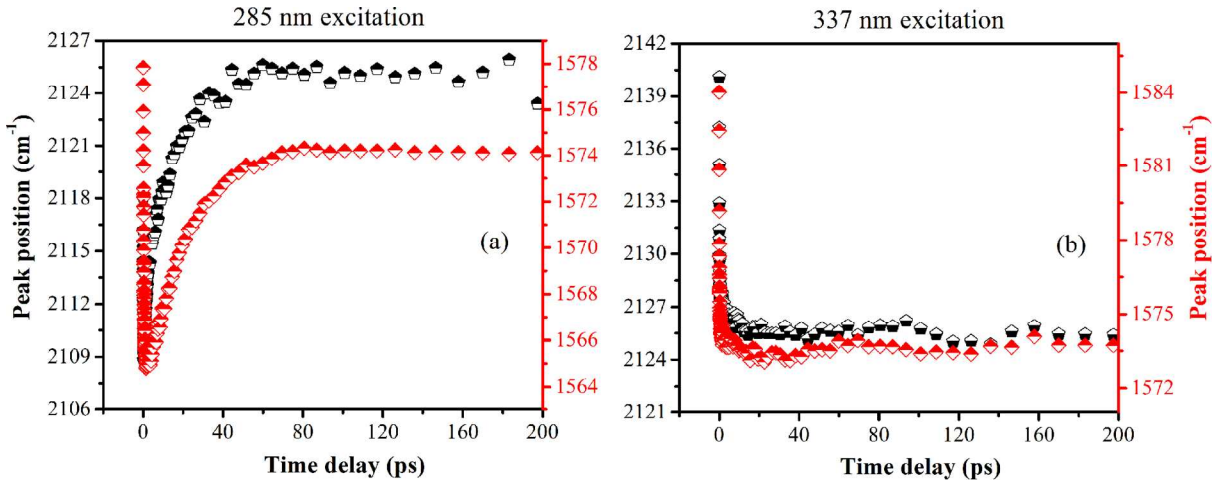

Figure 7. Time dependent peak positions of the CC double (right scales) and CC triple (left scale) bonds for 285 nm (a) and 337 nm (b) excitation.

Table 4. Excitation wavelength dependent time evolution (in ps) of the peak maxima of the CC triple and CC double bond stretch vibration in acetonitrile.

Excitation wavelength (nm)	CC triple bond str.		CC double bond str.	
	$\tau_{down\text{-}shift}$(ps)[a]	$\tau_{up\text{-}shift}$(ps)	$\tau_{down\text{-}shift}$(ps)[a]	$\tau_{up\text{-}shift}$(ps)
287	0.1	16	0.3	21
307[b]	0.2	12	0.4	20
337	0.1	----	0.1	----

[a]Shorter time constants are within the error limit of instrument time resolution, which is ±180 fs.
[b]Data shown for λ_{max}= 307 nm reproduced from ref 34.

Transient URLS spectra recorded at 337 nm excitation show very different results. Analysis of the peak positions for the high frequency vibrations of the CC double and CC

triple bonds shows only the initial redshift with a time constant of 0.1 ps. The long-lived component is practically flat, i.e. the peak positions do not show any change with delay time (>1 ps), as illustrated in figure. 7b. The parameters obtained from exponential fitting of the peak positions are given in Table 4 for different excitation wavelengths.

4. Discussion:

As discussed above, at room temperature BPEB exists as a mixture of various rotational conformers. At room temperature, it can exist as either planar, terminal rings twisted (TRT) or middle ring twisted (MRT) conformers.[72] These torsional conformers have a significant impact on the electronic absorption spectrum as well as the ultrafast excited state dynamics. In the ground state geometry, the normal mode frequency for the terminal ring twist is 12 cm^{-1} and for the central ring twist it is 40 cm^{-1} as obtained from DFT calculations using the B3LYP/cc-pVDZ level of method. It has been shown that the torsional angle has a dramatic effect on the S_0 and S_1 states.[72] Upon twisting of any ring from planarity, the potential energy for torsion increases gradually; the maximum torsional potential is found for 90˚ twists. Interestingly, the terminal ring twist and the middle ring twist correspond to different torsional potentials. According to the DFT-B3LYP (ground state) and TDDFT-B3LYP (excited state) calculations by Fujiwara *et al.*,[72] twisting of one of the terminal rings has much less effect on the torsional potential as compared to middle ring twist. For example, for a 30° twist of a terminal ring, the relative change in potential energy is ~100 cm^{-1} in the ground state, but for middle ring twist the change in potential energy is ~200 cm^{-1} (twice as high as expected).[72] Therefore, at room temperature, the extent of twisting would be larger for the terminal

rings in terms of torsional angle, whereas, for a middle ring the twisting angle is rather limited, since the relative torsional energy at 25˚C is equivalent to *kT* for such twists.[72] Temperature dependent absorption studies in solution phase show major changes with temperature: the room temperature absorption spectrum and the -198˚C absorption spectrum have completely different profiles.[38] At room temperature, the strongest peak appears around 316 nm and the second one appears at 337 nm, whereas at very low temperature the strongest peak appears at 337 nm and the second intense peak at ~320 nm. This agrees with the FC calculation of figure 3 (see also figure 1b). The sharp features observed in the low temperature absorption spectrum have been roughly assigned as vibronic bands of high frequency vibration with the help of spectral simulation. As shown in figures 1b & 3, at the longest possible pump wavelength we excite predominantly a subset of planar conformers.

Based on our femtosecond transient absorption results and computational studies it is evident that the S_1 excited state of BPEB exhibits three phases of excited state dynamics. We hypothesize that the three components observed in the TA experiment at 285 nm excitation could originate from different populations of conformers. We believe that the ultrafast component ~400 fs can be attributed to the middle ring twisted (MRT) species based on the following. It is known that the torsional barrier for the MRT conformer is around 6000 cm^{-1} (15 kcal/mole) in the excited singlet state[33,72] and upon Franck-Condon excitation from the ground state, MRT experiences a very steep potential in the S_1 surface, which causes it to relax very fast to a more planar geometry. As a result of the relatively low population in the ground state, only a fraction of the total number of excited molecules relaxes in this fashion, which is also evident from the decay associated

spectra in figure 5a. A second, relatively slow component also contributes to the rising of the transient signal until 50-60 ps. This could be due to the torsional relaxation of terminal ring twisted conformers (TRT). The terminal rings maintain a benzenoid structure even in the excited state, so the torsional barrier in this case is relatively low (and less steep) as compared to the excited MRT conformers.[72] Because of this lower torsional barrier TRT relaxes more slowly. From the decay associated spectra (figure 5a & 5b) it is evident that the concentration of such species (TRT, A2) is higher as compared to MRT (A1). The 285 nm actinic pump predominantly excites high energy twisted conformers which will experience a very steep potential in the S_1 state and consequently relax at ultrafast timescales. On the other hand, excitation with 337 or 347 nm primarily excites nearly planar conformers, resulting in slower decay kinetics as evident from the TA measurements. A 20 ps decay component with relatively small population contribution (see figure 5b. green, A2) is observed for the 347 nm excitation. This may be due to the planarization of a very small fraction of initially thermally activated TRT conformers. The slowest component corresponds to the decay of the fully relaxed S_1 species, which can originate from species that were near planar in the ground state and also from originally twisted species after S_1 relaxation. The absence of middle ring twisted structure is reflected in the species associated spectra (in figure 5b) which do not contain the ultrafast sub-picosecond component.

The vibrational energy relaxation of excited BPEB during its planarization is especially reflected in the high frequency Raman modes: the CC double and CC triple bond stretch vibrations. The initial fast down shift and slower up-shift of these high frequency vibrations are also discussed in our previous report.[34] The time constants obtained for 285

nm excitation are very similar as for 307 nm excitation. After 0-0 excitation at 337 nm, the shift in the transient URLS peak positions shows only the ultrafast downshift component. The origin of this downshift is attributed to the electronic delocalization along the conjugation coordinate after photo excitation, and this will also play a role for 285 nm and 307 nm excitations. Interestingly, the 2nd component (upshift), (which is assigned as vibrational relaxation coupled with torsional relaxation for 285 nm excitation) is completely absent in the case of 337 nm excitation. This is in agreement with the fact that the red edge excited sub-population exists almost exclusively as planar conformers. Furthermore, excitation into the red flank results in only very little excess energy, so there is no vibrational cooling observed for the high-wavenumber vibrations after 0-0 excitation, also in agreement with the unchanged full width at half maxima of the TA spectra in figure 4d-f.

5. Conclusion:

This report presents the direct observation of the excited state planarization dynamics of different conformational isomers of excited bis(phenylethynyl)-benzene. The effect of phenyl ring rotation on the absorption spectrum has been studied using computational methods. Franck-Condon analysis shows that the middle ring twist has a significant effect on the absorption spectrum as compared to the terminal-ring twist as calculated by Fujiwara *et al.*[72] Excitation wavelength dependent TA at the blue edge (285 nm) and red edge (347 nm) of the ground state absorption spectrum of BPEB clearly reveals the different dynamics of twisted and planar conformers. At 285 nm photo pump excitation, an ultrafast component was observed apart from two slower components. This

was attributed as decay of middle-ring twisted conformers, due to a very steep S_1 torsional potential. The second component with decay constant ~20-24 ps was assigned as excited BPEB with a terminal ring twisted structure. In contrast, the TA kinetics at 347 nm excitation does not show any ultrafast component; it has mostly the slower component originating from relaxation of (near-planar) structures. Excitation wavelength dependent transient URLS results provide important additional information: vibrational frequency shifts of high frequency vibrations behave differently for different sub-selections of conformers. From this study, we can conclude that one can have control over the conformational dynamics of molecular systems which could be useful in the field of opto-electronics.

Supporting Information:

The supporting information section contains the ground and excited states optimized geometries of 1,4-bis(phenylethynyl)benzene, along with HOMO-LUMO electron densities. Experimental kinetic traces of BPEB for 285 nm and 347 nm excitations and their global fitting curves.

Acknowledgements:

We thank the Council of Scientific and Industrial Research (CSIR) and the Department of Science and Technology (DST) for financial assistance. K. R & S.K. acknowledges CSIR for a research fellowship. S.U. acknowledges the DST for a J.C. Bose fellowship.

References:

(1) Brédas, J.L.; Chance, R. R. (Eds.), Conjugated Polymeric Materials: Opportunities in Electronics, Optoelectronics, and Molecular Electronics, ISBN 978-94-009-2041-5.

(2) Ostroverkhova, O. (Ed.), Handbook of Organic Materials for Optical and (Opto)electronic Devices Properties and Applications. A volume in Woodhead Publishing Series in Electronic and Optical Materials. ISBN: 978-0-85709-265-6.

(3) Chowdhary, P. D.; and Umapathy, S. Ultrafast dynamics and photochemistry of π- π^* excited trans-azobenzene: a comprehensive analyses of resonance Raman intensities. *J. Raman Spectrosc*. **2008**, 39, 1538-1555.

(4) Christina, M. S.; Frontiera, R. R.; Mathies, R. A. Excited-state structure and dynamics of cis- and trans-azobenzene from resonance Raman intensity analysis. *J. Phys. Chem. A* **2007,** 111, 12072-12080.

(5) Roland, T.; Heyer, E.; Liu, L.; Ruff, A.; Ludwigs, S.; Ziessel, R.; Haacke, S. A Detailed Analysis of Multiple Photoreactions in a Light-Harvesting Molecular Triad with Overlapping Spectra by Ultrafast Spectroscopy. *J. Phys. Chem. C* **2014**, 118, 24290-24301.

(6) Mohapatra, H.; Umapathy, S., Time-Resolved Resonance Raman Studies on Proton-Induced Electron Transfer Reaction from Triplet Excited State of 2-Methoxynaphthalene to Decafluoro Benzophenone. *J. Phys. Chem. A* **2010**, 114, 12447-12451.

(7) Mondal, S.; Puranik, M. Sub-50 fs Excited State Dynamics of 6-Chloroguanine upon Deep Ultraviolet Excitation. *Phys. Chem. Chem. Phys*. **2016**, 18, 13874-13887.

(8) Lednev, I. K.; Ye, T. Q.; Matousek, P.; Towrie, M.; Foggi, P.; Neuwahl, F. V. R.; Umapathy, S.; Hester, R. E.; Moore, J. N. Femtosecond Time-Resolved UV-Visible Absorption Spectroscopy of trans-Azobenzene: Dependence on Excitation Wavelength. *Chem. Phys. Lett*. **1998**, 290, 68-74.

(9) Kim, D.; Osuka, A. Photophysical Properties of Directly Linked Linear Porphyrin Arrays. *J. Phys. Chem. A* **2003**, 107, 8791–8816.

(10) Polkehn, M.; Tamura, H.; Eisenbrandt, P.; Haacke, S.; Méry, S.; Burghardt, I. Molecular Packing Determines Charge Separation in a Liquid Crystalline Bisthiophene–Perylene Diimide Donor–Acceptor Material. *J. Phys. Chem. Let*. **2016**, **7**, 1327-1334.

(11) Edwin, K.L.; Ghiggino, K.P. Electronic Energy Transfer in Multichromophoric Arrays. The Effects of Disorder on Superexchange Coupling and Energy Transfer Rate. *J. Phys. Chem. A* **2000**, 104, 5825-5836.

(12) Sahoo, S.; Umapathy, S.; and Parker, A. W. Time-Resolved Resonance Raman Spectroscopy: Exploring Reactive Intermediates. *Appl. Spectrosc*. **2011**, 65, 1087-1221.

(13) Biswas, N.; Umapathy, S. Study of Solvent Effects on the Molecular Structure and the Reorganization Energies of 4-Nitro-4′-Dimethylaminoazobenzene Using Resonance Raman Intensities. *J. Raman. Spec*. **2001**, 32, 471–480.

(14) Turro, N. J.; Ramamurthy, V.; Scaiano, J.C. Modern Molecular Photochemistry of Organic Molecules, University Science Books, Sausalito. **2010**.

(15) Umapathy, S.; Lee-Son, G.; Hester, R. E. Raman Spectroscopic Studies of Substituted Bipyridines, Their Ruthenium(II) Complexes and Surface-Derivatized TiO2. *J. Mol. Struct*. **1989**, 194, 107–116.

(16) Sung, J.; Kim, P.; Fimmel, B.; Wurthner, F.; Kim, D. Direct Observation of Ultrafast Coherent Exciton Dynamics in Helical π-Stacks of Self-Assembled Perlyene Bisimides. *Nat. Commun*. **2015**, 6, 8646-7.

(17) Wilson, T. M.; Tauber, M. J.; Wasielewski, M. R. Toward an n-Type Molecular Wire: Electron Hopping Within Linearly Linked Perylenediimide Oligomers. *J. Am. Chem. Soc.* **2009**, 131, 8952-8957.

(18) Ravi Kumar, V.; Ariese, F.; Umapathy, S. Triplet Excited Electronic State Switching Induced by Hydrogen Bonding: A Transient Absorption Spectroscopy and Time-Dependent DFT Study. *J. Chem. Phys*. **2016**, 144, 114301-8.

(19) Biswas, N.; Umapathy, S. Early Time Dynamics of *trans*-Azobenzene Isomerization in Solution from Resonance Raman Intensity Analysis. *J. Chem. Phys*. **1997**, 107, 7849-7858.

(20) Friend, R. H.; Gymer, R.W.; Holmes, A. B.; Burroughes, J. H.; Marks, R. N.; Taliani, C.; Bradley, D. D. C.; Santos, D. A. D.; Brédas, J. L.; Lögdlund, M.; Salaneck, W. R. Electroluminescence in Conjugated Polymers. *Nature* **1999**, 397,121-128.

(21) Bakulin, A. A.; Morgan, S. E.; Kehoe, T. B.; Wilson, M. W. B.; Chin, A.W.; Zigmantas, D.; Egorova, D.; Rao, A. Real-Time Observation of Multiexcitonic States in Ultrafast Singlet Fission using Coherent 2D Electronic Spectroscopy. *Nat. Chem*. **2016**, 8, 16-23.

(22) Alguire, E. C.; Subotnik, J. E.; Damrauer, N. H. Exploring Non-Condon Effects in a Covalent Tetracene Dimer: How Important are Vibrations in Determining the Electronic Coupling for Singlet Fission?. *J. Phys. Chem. A* **2015**, 119, 299–311.

(23) Mauck, C. M.; Brown, K. E.; Horwitz, N. E.; Wasielewski, M. R. Fast Triplet Formation via Singlet Exciton Fission in a Covalent Perylenediimide-β-Apocarotene Dyad Aggregate. *J. Phys. Chem. A* **2015**, 119, 5587–5596.

(24) Weiss, L. R.; Bayliss, S. L.; Kraffert, F.; Thorley, K. J.; Anthony, J. E.; Bittl, R.; Friend, R. H.; Rao, A.; Greenham, N. C.; and Behrends, J. Strongly Exchange-Coupled Triplet Pairs in an Organic Semiconductor. *Nat. Phys*. **2017**, 13, 176-181.

(25) Godin, R.; Wang, Y.; Zwijnenburg, M. A.; Tang, J.; Durrant, J. R., Time-Resolved Spectroscopic Investigation of Charge Trapping in Carbon Nitrides Photocatalysts for Hydrogen Generation. *J. Am. Chem. Soc*. **2017**. DOI: 10.1021/jacs.7b01547.

(26) Ojha, K.; Debnath, T.; Maity, P.; Makkar, M.; Nejati, S.; Ramanujachary, K. V.; Chowdhury, P. K.; Ghosh, H. N.; Ganguli, A. K. Exciton Separation in CdS Supraparticles upon Conjugation with Graphene Sheet. *J. Phys. Chem. C* **2017**. 121, 6581–6588.

(27) Perrin, M. L.; Frisenda, R.; Koole, M.; Seldenthuis, J. S.; Gil, J. A. C.; Valkenier, H.; Hummelen, J. C.; Renaud, N.; Grozema, F. C.; Thijssen, J. M.; Diana Dulić, D.; and van der Zant, H. S. J. Large Negative Differential Conductance in Single-Molecule Break Junctions. *Nat. Nanotech*. **2014**, 9, 830–834.

(28) Chen, J.; Reed, M. A.; Rawlett, A . M.; Tour, J. M. Large On-Off Ratios and Negative Differential Resistance in a Molecular Electronic Device. *Science* **1999,** 286, 1550-1552.

(29) Beeby, A.; Findlay, K. S.; Low, P. J.; Marder, T. B.; Matousek, P.; Parker, A. W.; Rutter, S. R.; Towrie, M. Studies of the S_1 State in a Prototypical Molecular Wire using Picosecond Time-Resolved Spectroscopies. *Chem. Commun*. **2003**, 2406-2407.

(30) Greaves, S. J.; Flynn, E. L.; Futcher, E. L.; Wrede, E.; Lydon, D. P.; Low, P. J.; Rutter, S. R.; Beeby, A. Cavity Ring-Down Spectroscopy of the Torsional Motions of 1,4-Bis(phenylethynyl)benzene. *J. Phys. Chem. A* **2006,** 110, 2114-2121.

(31) Levitus, M.; Schmieder, K.; Ricks, H.; Schimizu, K. D.; Bunz, U. H. F.; Garcia-garibay, M. A. Steps To Demarcate the Effects of Chromophore Aggregation and Planarization in Poly(phenyleneethynylene)s. 1. Rotationally Interrupted Conjugation in the Excited States of 1,4-Bis(phenylethynyl)benzene. *J. Am. Chem. Soc*. **2001**, 123, 4259-4265.

(32) Beeby, A.; Findlay, K.; Low, P. J.; Marder, T. B. A Re-evaluation of the Photophysical Properties of 1,4-Bis(phenylethynyl)benzene: A Model for Poly(phenyleneethynylene). *J. Am. Chem. Soc*. **2002**, 124, 8280-8284.

(33) James, P. V.; Sudeep, P. K.; Suresh, C. H.; Thomas, K.G. Photophysical and Theoretical Investigations of Oligo(p-phenyleneethynylene)s: Effect of Alkoxy Substitution and Alkyne−Aryl Bond Rotations. *J. Phys. Chem. A* **2006**, 110, 4329-4337.

(34) Roy, K.; Kayal, S.; Ariese, F.; Beeby, A.; Umapathy, S. Mode Specific Excited State Dynamics of Bis(phenylethynyl)-benzene from Ultrafast Raman Loss Spectroscopy. *J. Chem. Phys*. **2017**, 146, 064303-9.

(35) Castiglioni, C.; Zoppo, M. D.; Zerbi, G.; Vibrational Raman Spectroscopy of Polyconjugated Organic Oligomers and Polymers. *J. Raman Spectrosc*. **1993**, 24, 485–494.

(36) Hernandez, V.; Castiglioni, C.; Zoppo, M. D.; Zerbi, G. Confinement Potential and Pi -Electron Delocalization in Polyconjugated Organic Materials. *Phys. Rev. B. Condens. Matter***. 1994,** 50, 9815–9823.

(37) Milani, A.; Brambilla, L.; Zoppo, M. D.; Zerbi, G. Raman Dispersion and Intermolecular Interactions in Unsubstituted Thiophene Oligomers. *J. Phys. Chem. B* **2007**, 111, 1271–1276.

(38) Chu, Q.; Pang, Y. Vibronic Structures in the Electronic Spectra of Oligo(phenylene ethynylene): Effect of m-Phenylene to the Optical Properties of Poly(m-phenylene ethynylene). *Spectrochim. Spectrochimica Acta. Part A, Molecular and Biomol. Spectrosc*. **2004**, 60, 1459-1467.

(39) Lakshmanna, A.; Mallick, B.; Umapathy, S. Ultrafast Raman Loss Spectroscopy: A New Approach to Vibrational Structure. *Curr. Sci*. **2009**, 97, 210-216.

(40) Mallick, B.; Lakhsmanna, A.; Umapathy, S. Ultrafast Raman Loss Spectroscopy (URLS): Instrumentation and Principle. *J. Raman Spectrosc.* **2011**, *42*, 1883–1890.

(41) McCamant, D. W.; Kukura, P.; Yoon, S.; Mathies, R. A. Femtosecond Broadband Stimulated Raman Spectroscopy: Apparatus and Methods. *Rev. Sci. Instrum*. **2004**, 75, 4971-4980.

(42) Misawa, K.; Minoshima, K.; Kobayash, T. Femtosecond Inverse Raman Spectrum of Molecular J- Aggregates. *J. Raman Spectrosc.* **1995**, 26, 553-559.

(43) Dietze, D. R.; Mathies, R. A.; Femtosecond Stimulated Raman Spectroscopy. *Chem. Phys. Chem*. **2016**, 17, 1224-1251.

(44) Frontiera, R. R.; Mathies, R. A. Femtosecond Stimulated Raman Spectroscopy. *Laser & Photonics Rev*. **2011**, 5, 102–113.

(45) Kovalenko, S. A.; Dobryakov, A. L.; Ernsting, N. P. An Efficient Setup for Femtosecond Stimulated Raman Spectroscopy. *Rev. Sci. Instrum*. **2011**, 82, 063102-9.

(46) Roy, K.; Kayal, K.; Rai, N.; Umapathy, S. Femtosecond Stimulated Raman Scattering: Theory and Experiments. *Kiran, A Bulletin of Indian Laser Association* **2013**, 24, 8-11.

(47) Camant, D. W.; Kukura, P.; Mathies, R. A. Femtosecond Broadband Stimulated Raman: A New Approach for High-Performance Vibrational Spectroscopy. *Applied Spectrosc*. **2003**, 57, 1317-1323.

(48) Ploetz, E.; Marx, B.; Gilch, P. Origin of Spectral Interferences in Femtosecond Stimulated Raman Microscopy. *J. Raman. Spectros*. **2011**, 42, 1875-1882.

(49) Ariese, F., Roy, K., Ravi Kumar, V., Sudeeksha, H. C., Kayal, S. and Umapathy, S. Time-Resolved Spectroscopy: Instrumentation and Applications. *Encyclopedia of Analytical Chemistry*. **2017**, 1–55.

(50) Umapathy, S.; Roy, K.; Kayal, S.; Rai, N. K.; Kumar, V. R. Structure and Dynamics from Time Resolved Absorption and Raman Spectroscopy. *The Future of Dynamic Structural Science.* Chapter: Editors: J. A. K. Howard., H. A. Sparkes, P. R. Raithby, A.V. Churakov, Springer pp. **2014**, 25-42.

(51) Kukura, P.; McCamant, D. W.; Davis, P. H.; Mathies, R. A. Vibrational Structure of the S_2 (^1B_u) Excited State of Diphenyloctatetraene Observed by Femtosecond Stimulated Raman Spectroscopy. *Chem. Phys. Lett*. **2003**, 382, 81-86.

(52) Liebel, M.; Schnedermann, C.; Wende, T.; Kukura, P. Principles and Applications of Broadband Impulsive Vibrational Spectroscopy. *J. Phys. Chem. A*. **2015***,* 119, 9506-9517**.**

(53) Becke, A. D. Density-Functional Thermochemistry. III. The Role of Exact Exchange. *J. Chem. Phys*. **1993**, 98, 5648- 5652.

(54) Lee, C.; Yang, W.; and Parr, R. G. Development of the Colle-Salvetti Correlation-Energy Formula into a Functional of the Electron Density. *Phys. Rev. B* **1988,** 37, 785-789.

(55) Miehlich, B.; Savin, A.; Stoll, H.; and Preuss, H. Results Obtained with the Correlation Energy Density Functionals of Becke and Lee, Yang and Parr. *Chem. Phys. Lett* **1989**, 157, 200-206.

(56) Vosko, S. H.; Wilk, L.; and Nusair, M. Accurate Spin-Dependent Electron Liquid Correlation Energies for Local Spin Density Calculations: A Critical Analysis. *Can. J. Phys*. **1980**, 58, 1200-1211.

(57) Dunning Jr, T. H.; Gaussian Basis Sets for use in Correlated Molecular Calculations. I. The Atoms Boron Through Neon and Hydrogen. *J. Chem. Phys.* **1989**, 90, 1007-1023.

(58) Kendall, R. A.; Dunning Jr, T. H.; and Harrison, R. H. Electron Affinities of the First-Row Atoms Revisited. Systematic Basis Sets and Wave Functions. **1992**, 96, 6796-6806.

(59) Tomasi, J.; Mennucci, B.; and Cammi, R. Quantum Mechanical Continuum Solvation Models. *Chem. Rev*. **2005**, 105, 2999- 3093.

(60) Frisch, M. J.; Trucks, G. W.; Schlegel, H. B.; Scuseria, G. E.; Robb, M. A.; Cheeseman, J. R.; Scalmani, G.; Barone, V.; Mennucci, B.; Petersson, G. A.; *et al*. Gaussian 09, Revision C.01, Gaussian, Inc., Wallingford, CT, **2010**.

(61) Fursche, F.; and Ahlrichs, R. Adiabatic Time-Dependent Density Functional Methods for Excited State Properties. *J. Chem. Phys.* **2002**, 117, 7433- 7447.

(62) Scalmani, G.; Frisch, M. J.; Mennucci, B.; Tomasi, J.; Cammi, R.; and Barone, V.; Geometries and Properties of Excited States in the Gas Phase and in Solution: Theory and Application of a Time-Dependent Density Functional Theory Polarizable Continuum Model. *J. Chem. Phys.* **2006**, 124, 094107-15.

(63) Santoro, F.; Improta, R.; Lami, A.; Bloino, J.; and V. Barone, V. Effective Method to Compute Franck-Condon Integrals for Optical Spectra of Large Molecules in Solution. *J. Chem. Phys.* **2007**, 126, 084509-13.

(64) Santoro, F.; Lami, A.; Improta, R.; and Barone, V. Effective Method to Compute Vibrationally Resolved Optical Spectra of Large Molecules at Finite Temperature in the Gas Phase and in Solution. *J. Chem. Phys.* **2007**, 126, 184102-11.

(65) Barone, V.; Bloino, J.; Biczysko, M.; and Santoro, F. Fully Integrated Approach to Compute Vibrationally Resolved Optical Spectra: From Small Molecules to Macrosystems. *J. Chem. Theory and Comput.* **2009**, 5, 540-554.

(66) Puranik, M.; Umapathy, S,; Snijders, J. G,; and Chandrasekhar, J. Structure of the Triplet Excited State of Bromanil from Time-Resolved Resonance Raman Spectra and Simulation. *J. Chem. Phys*. **2001**, 115, 6106-6114.

(67) Rohrdanz, M. A.; Martins, K. M.; and Herbert, J. M. A Long-Range-Corrected Density Functional that Performs Well for both Ground-State Properties and Time-Dependent Density Functional Theory Excitation Energies, Including Charge-Transfer Excited States. *J. Chem. Phys*. **2009**, 130, 054112-8.

(68) Puranik, M.; Chandrasekhar,J.; Snijders, J. G .; and Umapathy, S. Time-Resolved Resonance Raman and Density Functional Studies on the Ground State and Short-Lived Intermediates of Tetrabromo-p-Benzoquinone. *J. Phys. Chem. A* **2001**, 105, 10562-10569.

(69) Mar, B. D.; Heather J. Kulik, H. J. Depolymerization Pathways for Branching Lignin Spirodienone Units Revealed with ab Initio Steered Molecular Dynamics. *J. Phys. Chem. A* **2017**, 121, 532-543.

(70) Puranik, M.; Chandrasekhar, J.; and Umapathy, S. Structure of the Triplet Excited State of Tetra-Bromoparabenzoquinone from Time-Resolved Resonance Raman Spectra and ab Initio Calculation. *Chem. Phys. Lett*. **2001**, 337**,** 224-230.

(71) Barone, V.; Bloino, J.; Biczysko, M. Vibrationally-Resolved Electronic Spectra in GAUSSIAN 09. 2009: GAUSSIAN 09 Revision A.02.

(72) Fujiwara, T.; Zgierski, M. Z.; Lim, E. C. Spectroscopy and Photophysics of 1,4-Bis(phenylethynyl)benzene: Effects of Ring Torsion and Dark πσ* State. *Phys. Chem. A.* **2008,** 112, 4736-4741.

Table of content graphics

The table of content graph shows probing of different conformational isomers of BPEB using three pulse ultrafast Raman loss spectroscopy experiments.

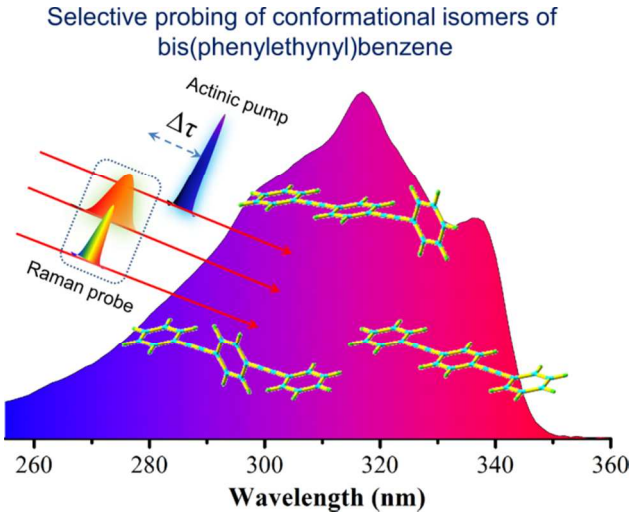

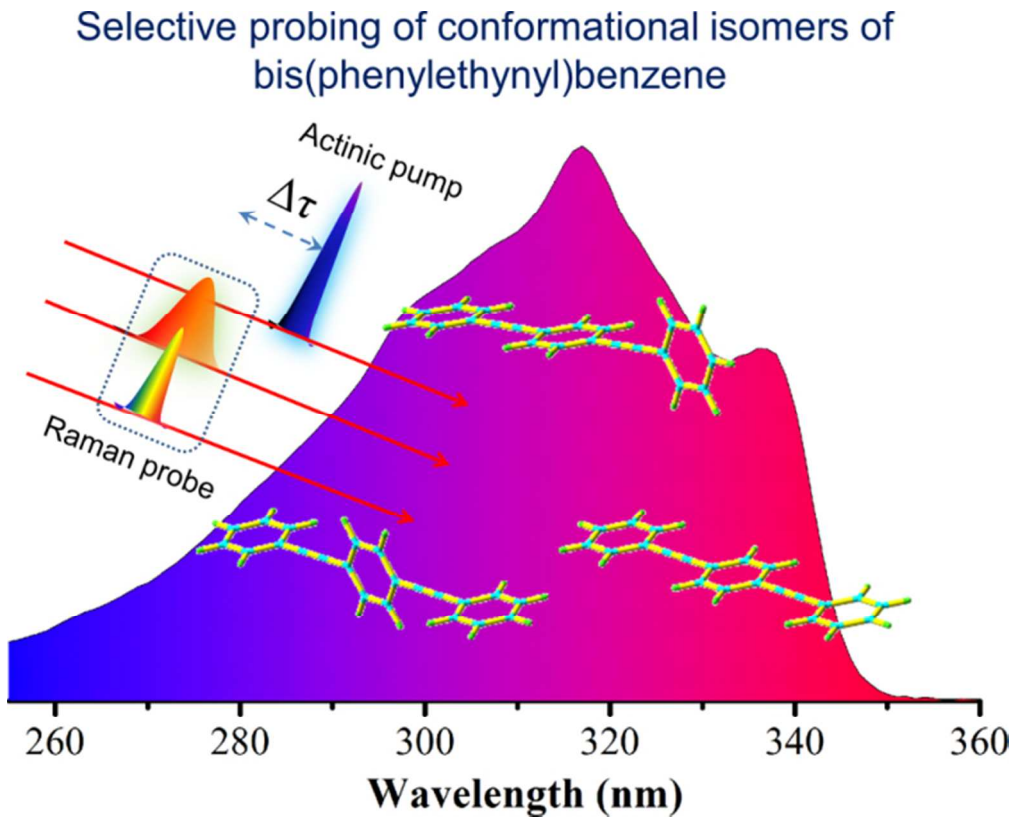

Table of Content Graphic

82x66mm (220 x 220 DPI)

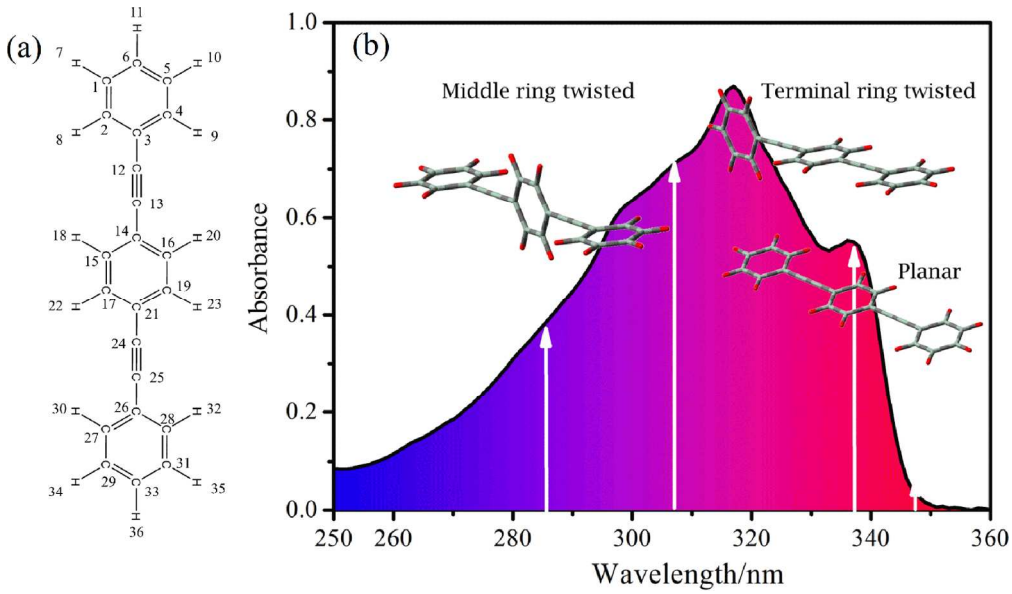

(a) Molecular structure of BPEB drawn in planar conformer. (b) Room temperature absorption spectrum of BPEB (20 μM in acetonitrile) showing the excitation wavelengths as discussed in this paper. The molecular tube structures illustrate the various twisted conformers. For selective excitation of the most planar conformers we used 337 nm for URLS and 347 nm for TA.

150x87mm (300 x 300 DPI)

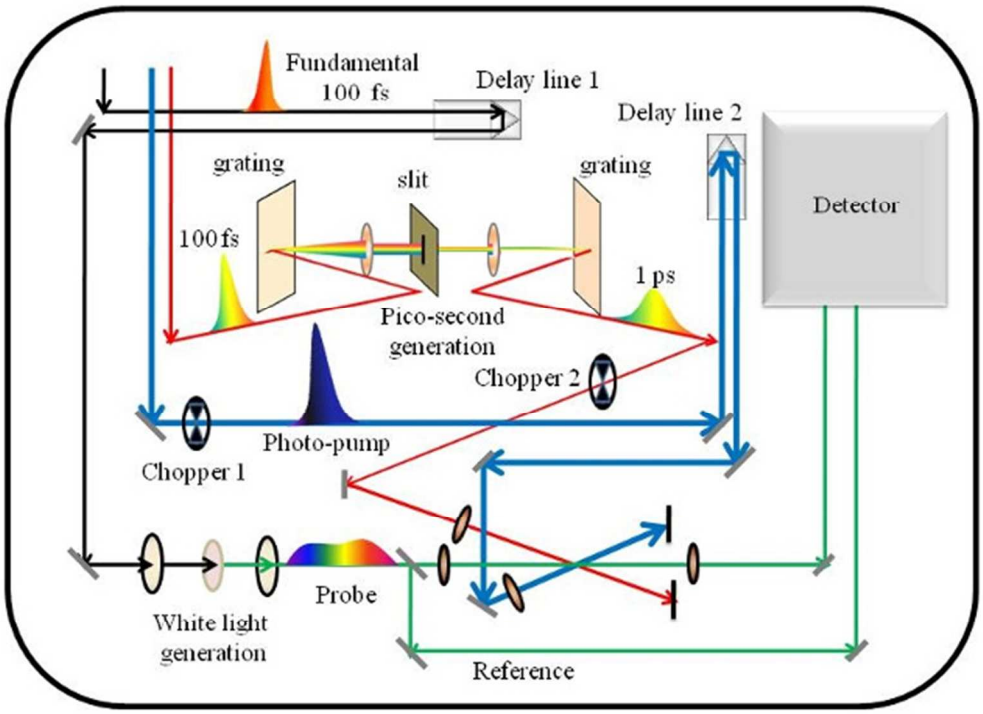

Schematic diagram of experimental set-up for femtosecond transient absorption and ultrafast Raman loss spectroscopy.

170x124mm (96 x 96 DPI)

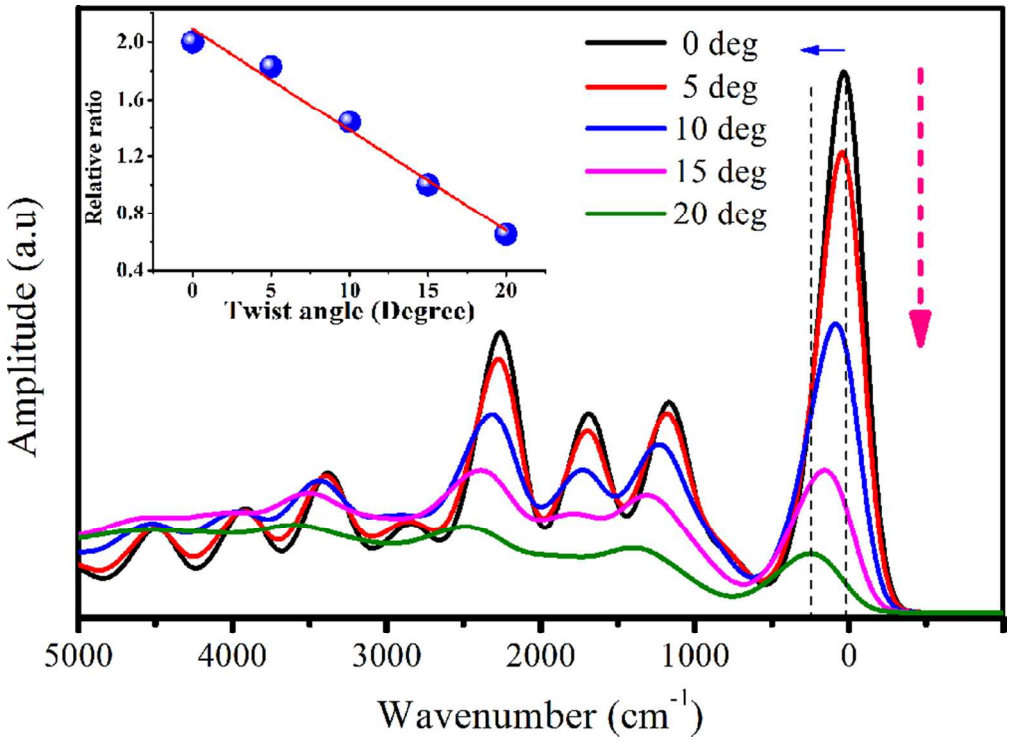

Simulated ground state absorption spectra of BPEB at increasing twist angles of the central ring. The x-axis shows the transition energy relative to the 0-0 transition of the planar species, found experimentally at 28902 cm^{-1} (346 nm). Inset shows the decrease in ratio of two most intense bands.

85x62mm (300 x 300 DPI)

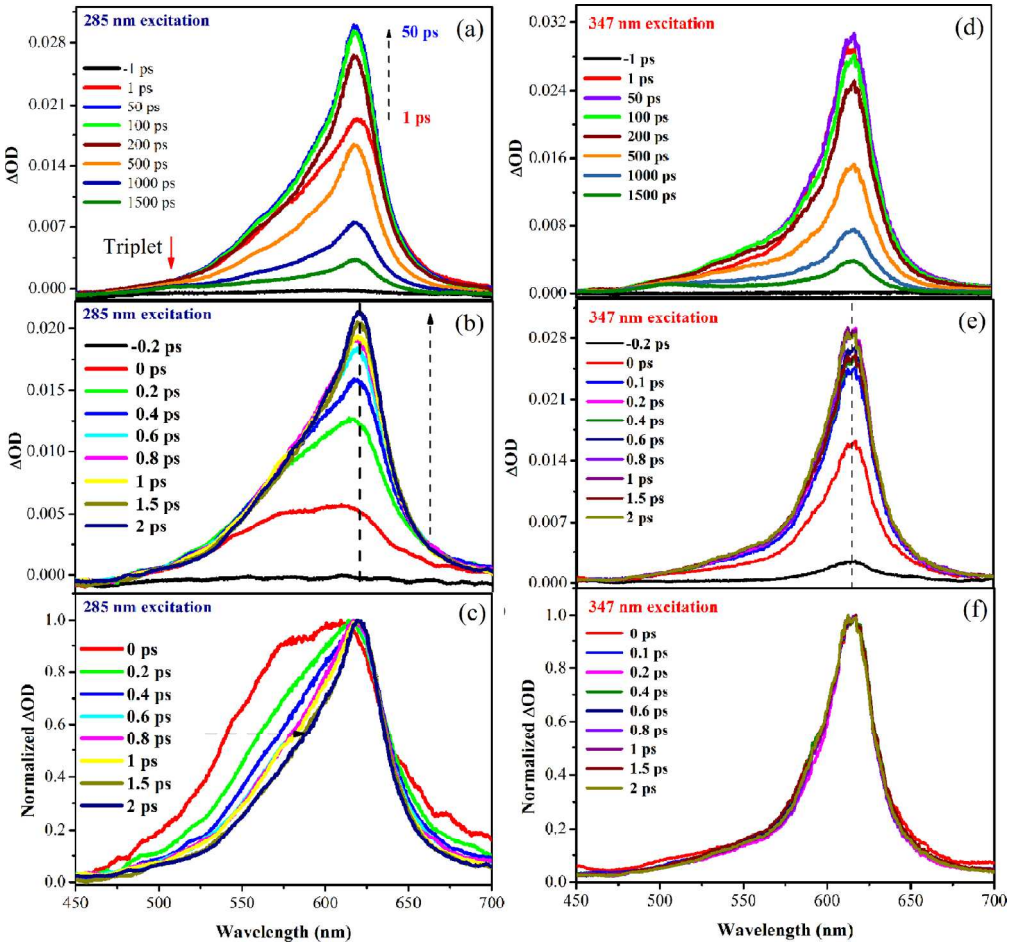

Femtosecond transient absorption spectra of BPEB for two different excitations are shown for longer (top) and shorter delays (middle). The latter are also shown after normalization (bottom frames).

170x159mm (300 x 300 DPI)

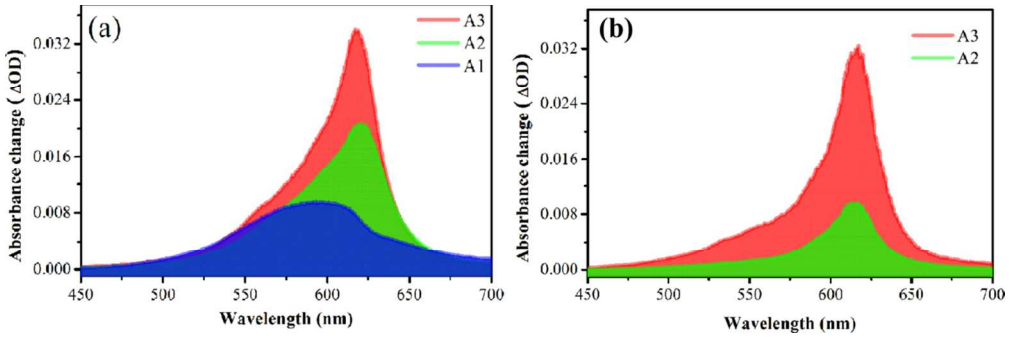

Species associated spectra of TA kinetics after global analysis using tri (285 nm exc, a) and bi (347 nm exc, b) exponential models.

160x52mm (220 x 220 DPI)

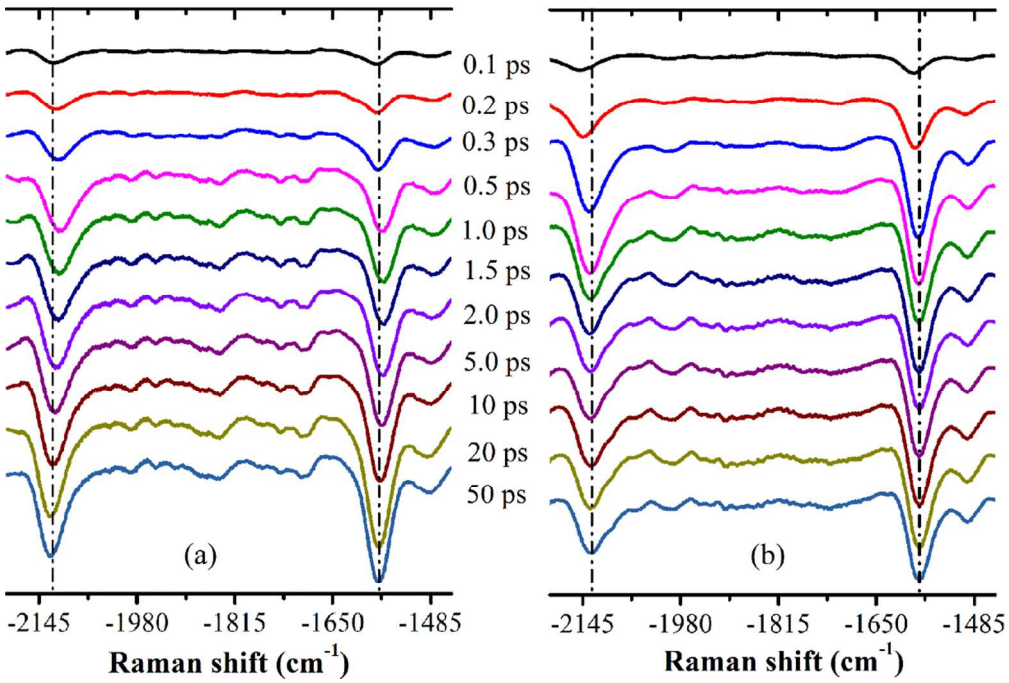

Transient Raman loss spectra of BPEB for 285 nm (a) and 337 nm (b) excitation wavelength at different time delays showing the CC double and triple bond stretches. Vertical lines are guides to the eye.

140x93mm (220 x 220 DPI)

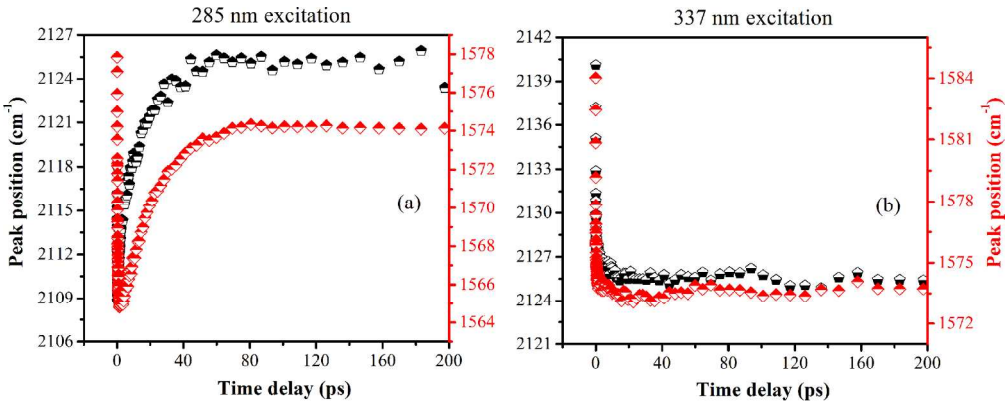

Time dependent peak positions of the CC double (right scales) and CC triple (left scale) bonds for 285 nm (a) and 337 nm (b) excitation.

177x69mm (300 x 300 DPI)